JOURNAL OF CATALYSIS 95, 361–369 (1985)

CO Desorption from Supported Ru Particles

C. PARK, W. G. DURRER, H. POPPA, AND J. T. DICKINSON[1]

Stanford/NASA–Ames Joint Institute for Surface and Microstructure Research, NASA–Ames Research Center, Moffett Field, California 94035

Received August 10, 1984; revised April 11, 1985

The low-pressure interaction of CO with small Ru particles supported on ultrahigh-vacuum-cleaved mica has been studied using flash thermal desorption, Auger electron spectroscopy, transmission electron microscopy, and transmission electron diffraction. Average particle size for these experiments varied between 1.2 and 6 nm. A careful search for CO decomposition on the Ru particles revealed no evidence for dissociation over pressure and temperature ranges of 10^{-11} to 10^{-6} Torr and 300 to 550°C, respectively. Gas and heat treatments caused significant changes in the morphology and dispersion of the Ru particles which in turn affected CO desorption. These effects were particle-size dependent.

INTRODUCTION

Ruthenium is an effective catalyst for a number of processes, including CO methanation and Fischer–Tropsch synthesis. Thus, there has been considerable interest in CO-interaction studies on both single-crystal surfaces (*1–6*) and supported small particles of Ru (*7, 8*). We present the results of studies of the interaction of CO with small Ru particles supported on ultrahigh-vacuum(UHV)-cleaved mica employing flash thermal desorption (FTD), Auger electron spectroscopy (AES), transmission electron microscopy (TEM), and transmission electron diffraction (TED). We were particularly interested in seeing if during repeated CO FTD cycles, we would observe the dissociation of CO that was observed earlier for Pd and Ni particles supported on mica (*9, 10*). As is discussed, our results show no evidence for CO dissociation on Ru particles. However, we present evidence for significant morphology changes of the particles induced by gas and heat treatments which affect CO desorption.

[1] Permanent address: Department of Physics, Washington State University, Pullman, Wash. 99164-2814.

EXPERIMENTAL

In a dual-chamber system, previously described (*9*), small Ru particles were vapor-grown onto high-purity mica (muscovite) that was heat-treated and cleaved in UHV. During vapor deposition the substrate temperature and metal flux were held constant at 270°C and 0.20 nm/min, respectively. The metal flux was measured with a quartz-crystal microbalance positioned such that a 1-Hz change in the crystal oscillation frequency corresponded to 0.02 nm of Ru deposited on the sample. The pressure during deposition was less than 5×10^{-9} Torr, with H_2, CO, and H_2O being the principal species. Deposition times ranged from 30 to 300 sec. The samples were analyzed by AES to determine the relative metal coverages and the presence of contamination. Successive FTDs of CO were used to observe the chemisorption properties of the particles and to assess changes which occur as a result of thermal desorption cycling and other gas–thermal treatments. All CO desorptions were accomplished by rapidly inserting the sample into a cylindrical oven which was held at a temperature of 370°C. The surface temperature versus time was

0021-9517/85 $3.00

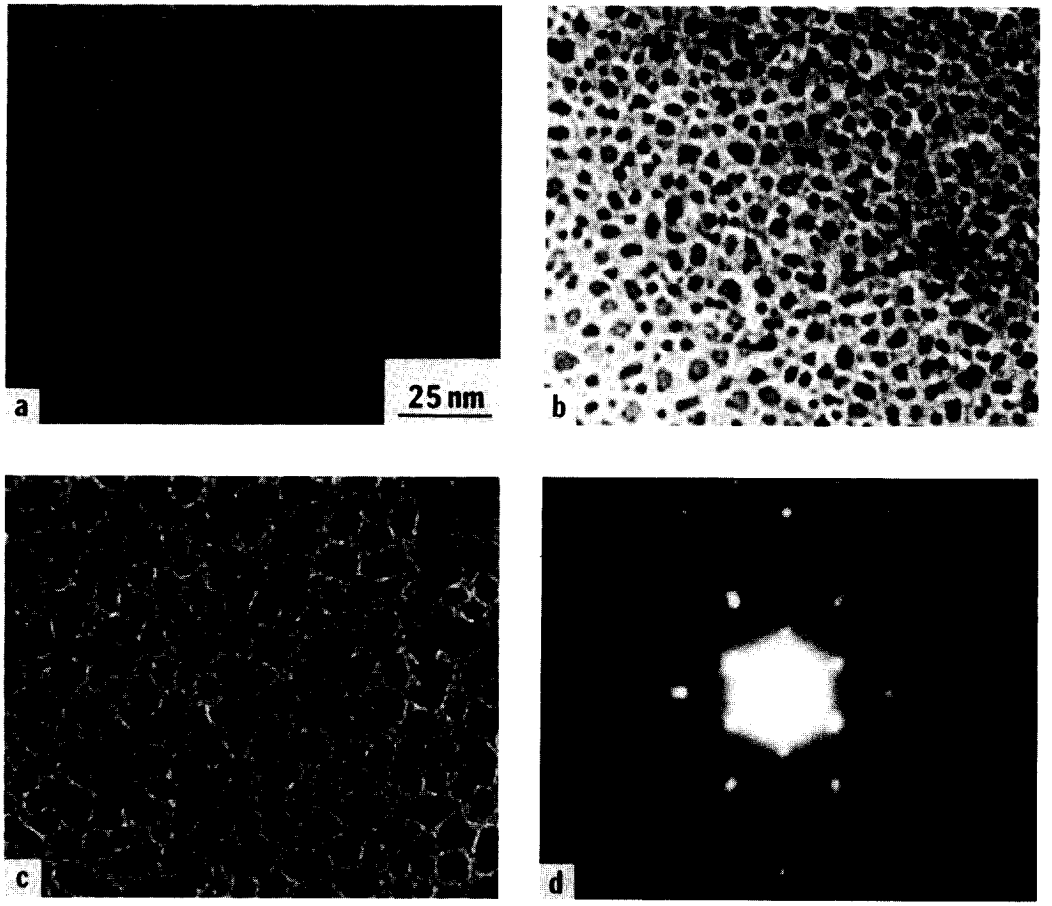

FIG. 1. Transmission electron micrographs of as-deposited particulate Ru films. (a) 30-sec/5-Hz deposit: average particle diameter, $\langle d \rangle = 1.2$ nm, particle number density, $n = 3.7 \times 10^{12}/\text{cm}^2$. (b) 150-sec/25-Hz deposit: $\langle d \rangle = 2.8$ nm, $n = 3.4 \times 10^{12}/\text{cm}^2$. (c) 300-sec/50-Hz deposit: $\langle d \rangle = 6.0$ nm, $n = 1.3 \times 10^{12}/\text{cm}^2$. (d) TED pattern for deposit (b). The sharp reflections are due to diffraction from the mica. The more diffuse and slightly arched spots with sixfold symmetry are from Ru; they are in good registry with the mica pattern, indicating strong epitaxy.

deduced from earlier temperature calibrations using thermocouples embedded into the mica (*11*). The CO desorption flux was monitored by a quadrupole mass spectrometer placed in direct line-of-sight of the specimen through a hole in the oven wall. Auger spectra were taken immediately after the desorption of CO ($P_{CO} < 1 \times 10^{-9}$ Torr) to avoid CO adsorption from background CO and to prevent electron-beam-induced contamination of the particle surfaces. After a set of samples was tested, the specimens were removed from the UHV system and evaluated by TEM–TED.

RESULTS

Transmission electron microscopy and diffraction. As-deposited samples, without further gas or thermal treatments, were examined by TEM and found to have average particle diameters ranging from 1.2 to 6 nm for deposition times of 30 to 300 sec. Figures 1a–d show representative micrographs for the Ru deposits. The particle number density ranged from 1.3×10^{12} to $3.7 \times 10^{12}/\text{cm}^2$. For an equivalent metal deposit thickness, the Ru particles on mica are smaller and have a higher number density when

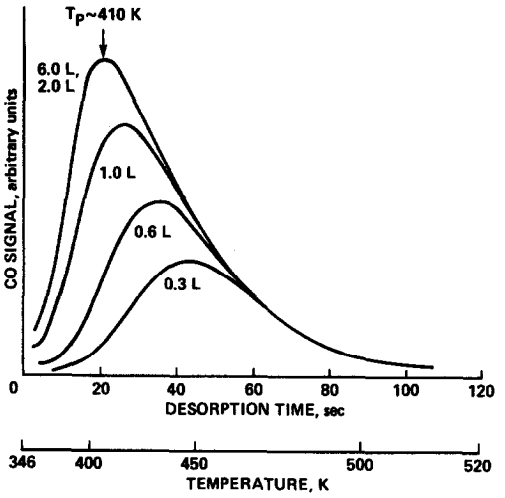

FIG. 2. CO desorption spectra for a series of CO exposures on a 150-sec/50-Hz Ru deposit. The CO adsorption temperature was 320 K (T_p = temperature of desorption peak maximum after saturation CO dose).

compared with Pd/mica (*9*). This increased nucleation rate suggests an increased interaction between Ru and mica. TED patterns showed all depositions to have hexagonal close-packed (hcp) structure. Structural modification to face-centered cubic (fcc), which was observed in the case of small Gd particles (*12*), was not detected here. TED showed that all depositions exhibited a high degree of epitaxy (see Fig. 1d). The observed epitaxial relationships, expressed in terms of standard crystallographic Miller indices, were $\langle 10\bar{1}0\rangle_{Ru}//\langle 020\rangle_{mica}$ or $\langle 130\rangle_{mica}$ and $\langle 22\bar{1}0\rangle_{Ru}//\langle 200\rangle_{mica}$. The particles were predominantly oriented with the Ru (001) direction normal to the mica surface. The exposed crystal faces depended on the three-dimensional particle shapes which are not directly discernible from TED; from surface free energy considerations, one would expect predominantly [101] and [001] facets.

CO DESORPTION SPECTRA

Typical desorption spectra for a 25-Hz (0.5-nm nominal thickness) deposit as a function of CO exposure are shown in Fig. 2. When assigning a temperature scale to these curves, the shapes and changes with CO exposure are consistent with first-order desorption with a coverage-dependent activation energy. From the peak position of the low-coverage FTD spectrum, we then calculate an activation energy of 35 kcal/mole, assuming a preexponential factor of 10^{+16} sec^{-1}, as suggested by Pfnuer *et al.* (*13*). (If the usual factor of 10^{+13} sec^{-1} is used, an activation energy of 29 kcal/mole results.)

The initial spectra for saturated CO dose (6 L) and three different particle sizes [(1) 1.2-nm, (2) 2.8-nm, and (3) 6.0-nm average diameters] are shown in Fig. 3. As expected, the increasing metal surface area produces more desorbed CO. Normalizing these curves to the same peak height showed that the peak shape and positions did not differ significantly over this range of particle size. Single-crystal studies of CO desorption from a number of different crystal faces show an appreciable amount of structure sensitivity for CO desorption peak shape (*3, 5, 30, 31*). Our results, therefore, suggest that the three-dimensional shapes of the particles remained rela-

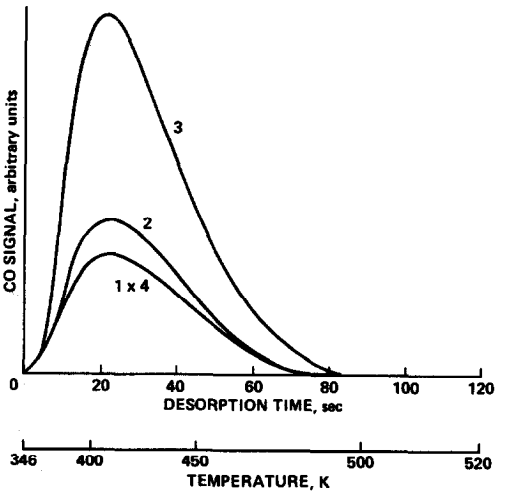

FIG. 3. Initial CO desorption spectra for different average-particle-size Ru deposits: (1) 1.2, (2) 2.8, and (3) 6.0 nm. All CO exposures were 6.0 L. Curve (1) has been magnified by a factor of 4 to better show its shape and peak position.

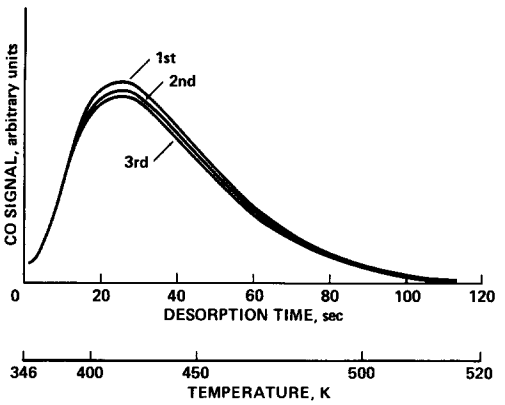

FIG. 4. Three successive CO FTD spectra for a 300-sec/50-Hz Ru deposit of $\langle d \rangle$ = 6.0 nm; CO dose = 6.0 L.

tively constant for these various conditions.

1. Search for CO Decomposition

A careful search for evidence of CO decomposition on small Ru particles produced by CO adsorption/desorption cycles was carried out by (a) measuring successive CO FTD spectra and looking for decay in peak height and peak area owing to carbon buildup (if loss of peak area by particle sintering and/or reconstruction can be excluded), and (b) performing AES measurements on the supported particles after each FTD in an attempt to detect C contamination. Figure 4 shows a typical set of successive spectra recorded using 6-L saturation doses of CO. Only slight asymmetric losses of area, mainly on the high-temperature sides of the first few desorptions, were observed. This is in contrast to previous results for Pd and Ni particles on mica (*9*, *10*) in which 30–70% area losses were found. (In some cases we did observe a significant decay of FTD area on Ru; however, these decays were caused by small amounts of coadsorbed oxygen due to an accidental, small leak in our vacuum system. Once this leak was eliminated, all significant FTD area losses vanished.)

We also looked for particle coalescence effects during repeated CO FTD cycles because coalescence with sintering would lead to surface area losses and would thus cause FTD peak area losses. TEM micrographs of Ru deposits that had or had not experienced several FTD cycles were compared for this purpose. Measurements of particle size and number density showed no significant change, suggesting that the observed small decrease in CO surface area cannot be attributed to sintering.

In addition, a careful search for the presence of carbon using high-sensitivity AES was carried out, although this was hampered by difficulties caused by C/Ru spectra overlap. Difference curves of the Ru (273 eV) peak before and after several FTD cycles, as well as measurements of ratios of the Ru (273 eV) to the Ru (231 eV), and to the Ru (200 eV) peaks, yielded no evidence of C. We therefore conclude from these results that at least for the surface coverages and temperatures of our experiments, no C buildup on the Ru particles was observed within our detection limit; consequently, there is no evidence for CO dissociation on Ru particles. We are thus led to the conclusion that the minor loss of FTD peak area occurring with repeated CO FTD cycles is due only to morphological particle changes or to minor particle/support interactions that occur during CO adsorption–desorption cycling.

2. Effect of Steady-State Heat Treatment

The changes induced by extended-time heat treatments were examined by FTD and TEM. After a first CO FTD cycle, the sample was annealed at 350°C for 35 min and cooled to 50°C, and then a second FTD cycle was carried out. Additional anneals followed by a CO adsorption/desorption cycle were performed. The results for a 5-Hz deposit are shown in Fig. 5a, in which a decrease in peak area with successive flashes is obvious. Note the distinct, asymmetric decrease on the high-energy side of the peak, suggesting that annealing reduces the concentration of high-energy binding sites for CO. It was also found that the rate

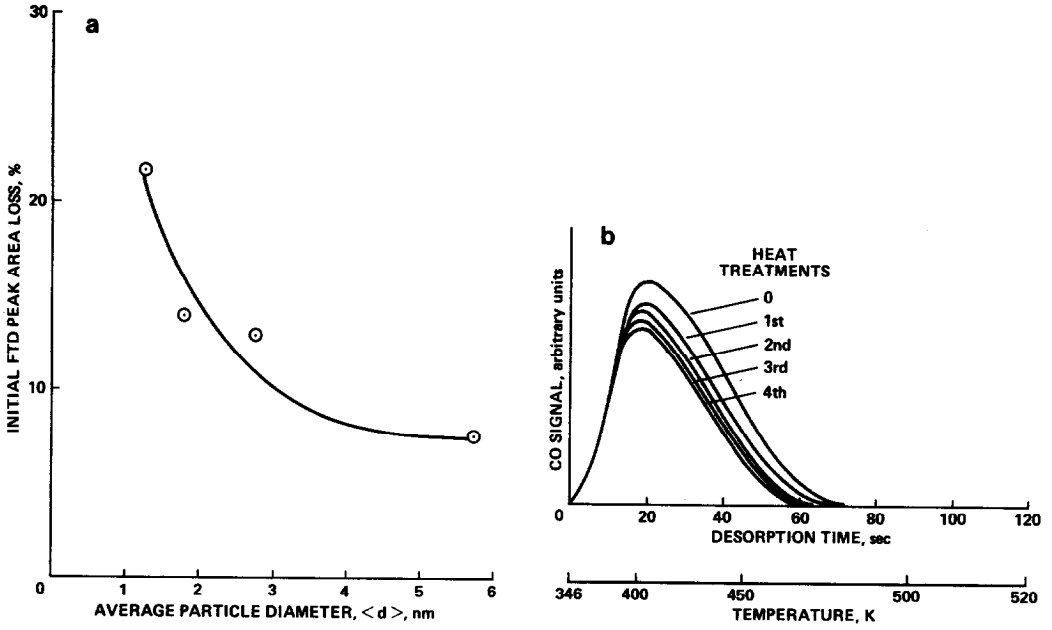

FIG. 5. (a) Effect of repeated heat treatments (350°C, 35 min) on the CO desorption spectra for a 30-sec/5-Hz Ru deposit; CO dose = 6.0 L. (b) Decay induced by heat treatment (350°C, 35 min) in CO FTD peak area (in percentage FTD peak area loss per flash) versus particle size.

of decay in FTD peak area with successive flashes is strongly particle-size-dependent as shown in Fig. 5b. As discussed in the next section, we attribute these annealing effects to a combination of particle coalescence and faceting. The TEM evidence for the latter is very strong, as seen in Fig. 6 for deposits before and after heat treatment. We see that the particles are transformed from irregular shapes (Figs. 6a and b) to more clearly defined hexagonal shapes (Figs. 6c and d). Such changes are accompanied by a reduction in surface irregularities such as steps, kinks, edges, and corners which are usually correlated with lower coordination surface atoms with higher adsorption energy.

3. *Effect of O_2 Preexposure*

When a CO FTD cycle included a 0.3-L predose of O_2 (5×10^{-9} Torr for 60 sec) at room temperature, the resulting FTD curves (see Fig. 7) showed a clear asymmetric decrease, similar to the peak decay observed upon annealing (Fig. 5b). With increasing amounts of predosed O_2, the CO FTD peak height decreased further and the peak shifted substantially toward the lower-temperature side; CO adsorption eventually was totally blocked by 6 L oxygen as can be seen in Fig. 7. Such a strong peak shift to a lower temperature suggests a substantial decrease of the CO binding energy in the remaining adsorption sites, the higher-energy sites presumably being occupied by oxygen.

However, this CO peak decay was partially reversible; about 90% of the original peak area could be recovered by the standard heat treatment (300°C for 35 min). O_2 desorption could not occur at this temperature (the activation energy for O_2 desorption is approximately 80 kcal/mole) (*2*, *14*). Oxygen removal by background CO to form CO_2 can also be dismissed because the CO oxidation rate at 300°C and CO pressures even as high as 10^{-7} Torr is still very low (*14*). In spite of this, an attempt was made to observe the CO_2 reaction directly by producing a high CO background pressure of 1

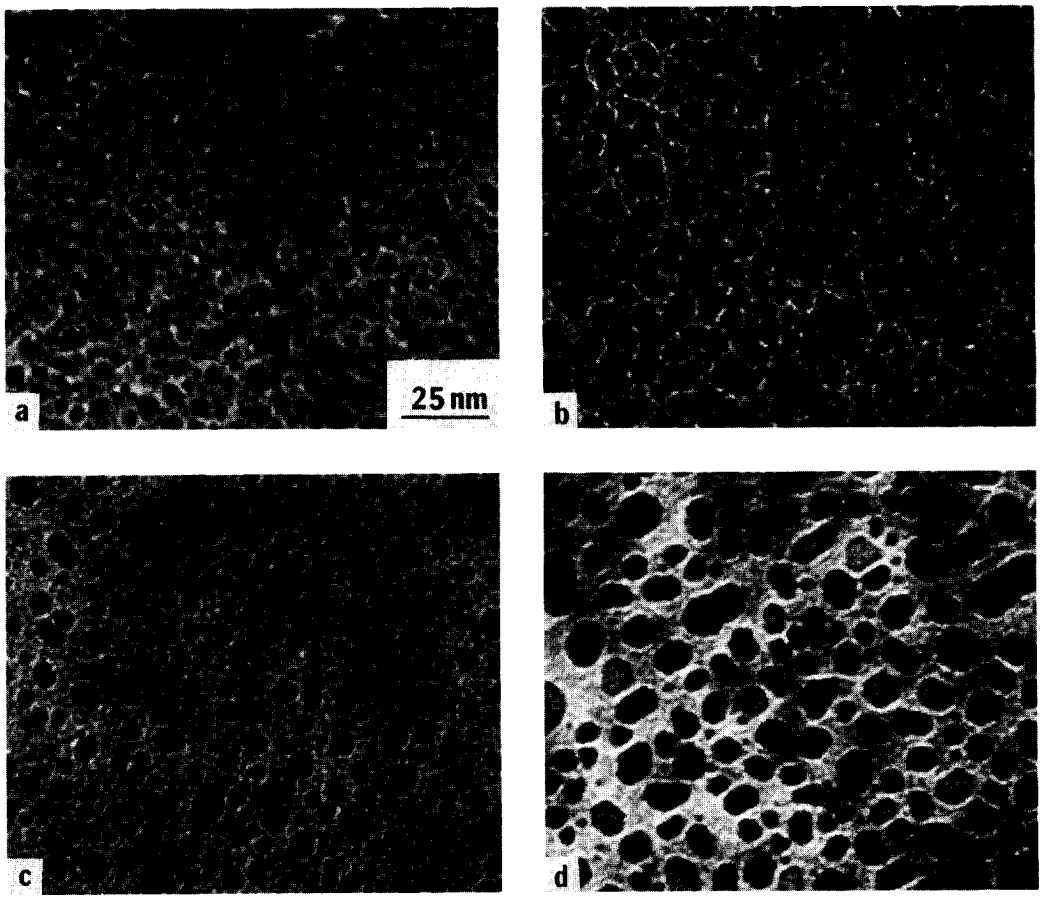

FIG. 6. Pairs of transmission electron micrographs illustrating the sintering effect of a heat treatment (350°C, 35 min) on the Ru particles for two deposits: (a) → (c) 150 sec, 25 Hz; (b) → (d) 300 sec, 50 Hz.

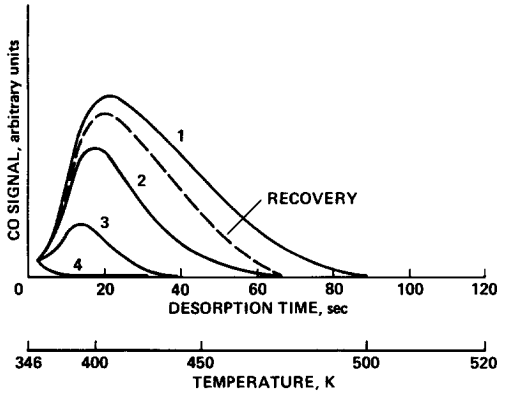

FIG. 7. The effect of O_2 preexposure on standard (6 L) FTD spectra for a 30-sec/5-Hz Ru deposit for: (1) no O_2 (6 L), (2) 0.3 L of O_2, (3) 3 L of O_2, and (4) 6 L of O_2. Curve (4) (dashed) peak recovery produced by a heat treatment of 35 min at 350°C, CO (6 L).

$\times 10^{-7}$ Torr during standard (300°C) heat treatment, but no CO_2 was detected. As discussed later, a possible fate of the oxygen is diffusion into the bulk of the Ru particles.

However, when the Ru particles were exposed to oxygen at high temperatures, the FTD area losses were irreversible. During an exposure of a clean Ru/mica sample to 5 $\times 10^{-9}$ Torr O_2 at 350°C for 35 min, the particles were permanently poisoned, incapable of adsorbing any CO. We suspect that the heated particles become partially oxidized when exposed to oxygen.

The TEM results for particles heat-treated in O_2 at 5 $\times 10^{-9}$ Torr and at 350°C for 30 min (see Fig. 8) support the surface oxidation hypothesis. All TED patterns

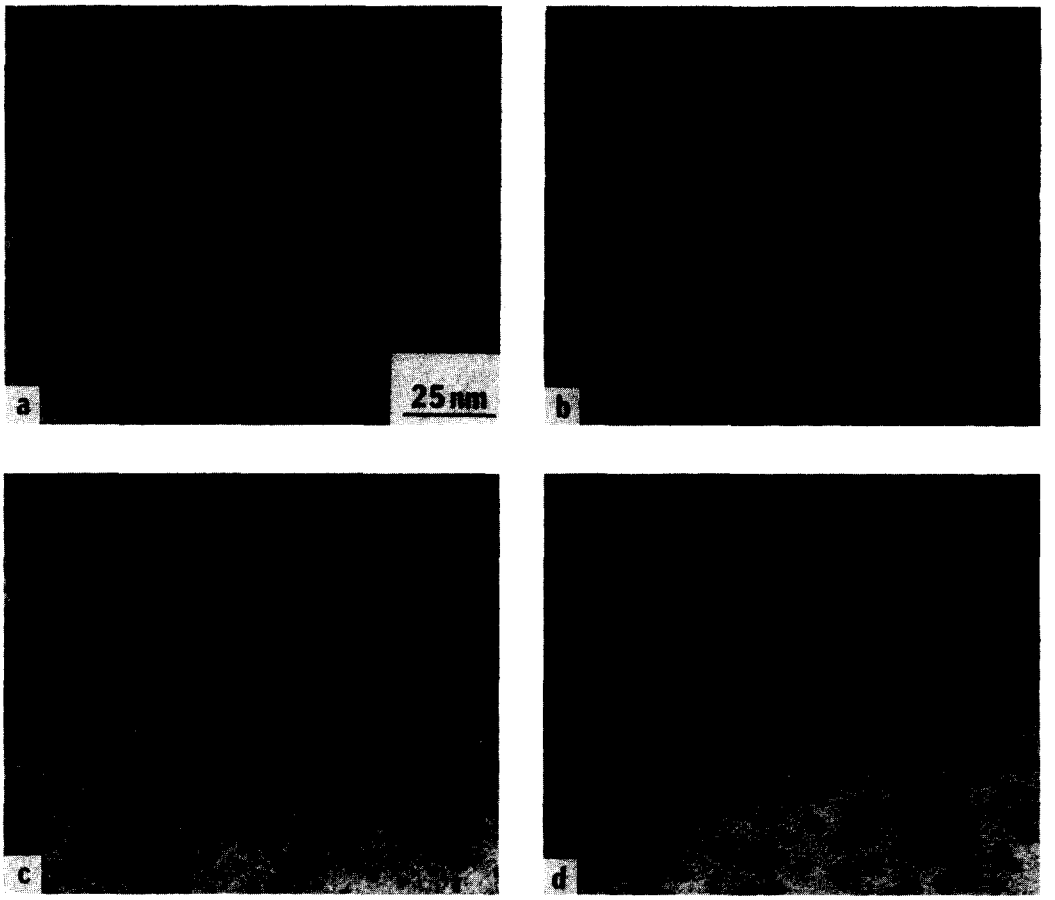

FIG. 8. Transmission electron micrograph showing the effect of heat treatment in O_2 (1×10^{-7} Torr for 35 min at 350°C) for two Ru deposits: (a) → (c) 60 sec, 10 Hz; (b) → (d) 150 sec, 25 Hz.

showed Ru reflections only, and no Ru/oxide rings were detected. The possibility of bulk oxidation is therefore excluded. However, the particles are spreading out more over the mica surface (wetting). Particulate surface oxidation accompanied by increased wetting of an oxide support has been reported for Ni/mica (*9*), Fe/Al_2O_3 (*15*), Pt/Al_2O_3 (*16*), Ir/SiO_2, (*17*), and Pd/MgO (*18, 19*).

DISCUSSION AND CONCLUSIONS

The lack of evidence for CO decomposition at low CO pressure on Ru particles supported on mica is similar to the case of Pt/mica (*20*), but contrary to what was observed for Ni/mica (*9*) and Pd/mica (*10*). For Pd and Ni, the strong particle-size effect was attributed to the high density of edge and corner sites (low-coordination sites) on small particles. The same type of sites presumably are also present on evaporated Pt and Ru particles, yet no dissociation of CO was observed. This observation for Ru disagrees with the general criteria for predicting CO dissociation as proposed by Broden *et al.* (*21*), where one orders the transition metals according to their tendency to dissociate CO (as predicted from photoemission studies of adsorbed CO). Ni and Pd are further removed from the region of transition between low and high CO dissociation tendency than Ru. Thus, contrary to the results of this study, we would ex-

pect Ru to have a greater tendency to decompose CO than either Ni or Pd.

The pronounced particle-size dependence of CO decomposition seen on Pd and Ni, and the fact that no CO decomposition was observed on low-index single-crystal surfaces of Pd and Ni suggest that CO decomposition occurs on sites that differ substantially from those on single-crystal surfaces. CO chemisorption bonding is generally explained by the donor–acceptor mechanism [Blyholder model (*22, 23*)], in which the bond is formed through electron transfer from the highest filled orbital of CO (*5*) to the metal and by "back donation" of metal electrons to the lowest unfilled orbital of CO. This electron transfer into the $2\pi^*$ orbitals can cause appreciable weakening of the carbon–oxygen bond (*24*). The "special" sites could conceivably lead to CO decomposition through their greater ability to weaken the carbon–oxygen bond via an increased back-donation of electrons. Whether the types and numbers of such sites on small Ni, Pd, Pt, and Ru particles are of comparable nature is an open question at this point because possible differences in microstructure and habits have not been sufficiently characterized. If similar particle habits are assumed, however, the density and types of special sites on particles of comparable size should be similar (*24*). The discrepancies in the tendencies of the various group VIII metals to decompose CO would then have to be ascribed to the differing electronic structures of the various metals or to different metal–support interactions.

A survey of previous work on CO decomposition on Ru introduces another aspect of the interpretation of our results, namely, CO pressure. Goodman *et al.* (*4*) could not detect any surface carbon after heating a Ru (110) surface to 630 K at a CO pressure of 2×10^{-3} Torr for 30 min, and Madey *et al.* (*1*) observed no detectable CO dissociation on Ru (001) at temperatures and pressures as high as 700 K and 10^{-4} Torr, respectively. In high-pressure experiments, on the other hand, Singh and Grenga (*25*) have reported carbon deposition on a polycrystalline Ru sphere exposed to 760 Torr of CO at 550 K, and Goodman *et al.* (*26*) more recently reported carbon deposition from CO on a Ru (110) surface exposed to 24 Torr of CO. Also, Low and Bell (*7*) found disproportionation of CO at high pressure (1 atm) during CO desorption on supported Ru particles on alumina. Rabo *et al.* (*27*) observed similar disproportionation of CO on a Ru/SiO_2 system, and McCarty and Wise (*8*) showed in an isotopic exchange study dissociative chemisorption of CO at high pressure on alumina-supported Ru particles. These results indicate that CO pressure may be an important factor in the decomposition of CO on Ru.

All particle sizes studied here showed an asymmetric decrease of the CO FTD peak following the various heat treatments, owing to the loss of higher-energy binding sites. The TEM data added clear evidence of faceting during heat treatment, which also implies the reduction of lower coordination surface sites. This conclusion is consistent with Wulff's theorem (*28*) that particles will facet in ways to reduce the total surface free energy of the particles as they approach their equilibrium structure. The strong particle-size dependence of these changes is probably caused by enhanced particle mobility on the support surface and particle refaceting (surface self-diffusion).

The loss of surface oxygen and the subsequent revival of the CO desorption peak during annealing of previously oxygen-dosed particles is also noteworthy. We speculate that during heat treatment, oxygen (chemisorbed at 50°C) diffuses into the bulk of the Ru, producing clean Ru sites capable of CO adsorption. This type of oxygen diffusion has been observed on single-crystal Ru by Reed *et al.* (*2*) and Lee *et al.* (*29*).

In summary, we observed no evidence of CO decomposition on particulate deposits of Ru on mica at pressures of 10^{-11} to 10^{-6}

Torr and temperatures of 300 to 550 K, respectively. However, we did observe significant changes in particle morphology and degree of particle dispersion induced by gas and heat treatments which strongly influence the adsorption and desorption of CO from supported Ru.

ACKNOWLEDGMENTS

We thank Dr. Dale Doering and Dr. Miguel Avalos-Borja for their assistance in these experiments, and Dr. Klaus Heinemann and Dr. Patrick Pizzo for their helpful comments. Funds for the support of this study have been allocated by NASA–Ames Research Center under Interchanges NCA-OR840-002 and NAC-OR840-102 and Cooperative Agreement NCC2-193.

REFERENCES

1. Madey, T. E., and Menzel, D., *Jpn. J. Appl. Phys. Suppl.* **2,** 229 (1974).
2. Reed, P. D., Comrie, C. M., and Lambert, R. M., *Surf. Sci.* **59,** 33 (1976).
3. Fuggle, J. C., Umbach, E., Feulner, P., and Menzel, D. M., *Surf. Sci.* **64** (1977).
4. Goodman, D. W., Madey, T. E., Ono, M., and Yates, J. T., Jr., *J. Catal.* **50,** 279 (1977).
5. Ku, R., and Gjostein, N. A., *Surf. Sci.* **64,** 465 (1977).
6. Thomas, G. E., and Weinberg, W. H., *J. Chem. Phys.* **70,** 1437 (1979).
7. Low, G. G., and Bell, A. T., *J. Catal.* **57,** 397 (1979).
8. McCarty, J. G., and Wise, H., *Chem. Phys. Lett.* **61,** 323 (1979).
9. Doering, D. L., Dickinson, J. T., and Poppa, H., *J. Catal.* **73,** 91 (1982).
10. Doering, D. L., Poppa, H., and Dickinson, J. T., *J. Catal.* **73,** 104 (1982).
11. Thomas, M., Dickinson, J. T., Poppa, H., and Pound, G. M., *J. Vac. Sci. Technol.* **15,** 568 (1978).
12. Morozov, Uy G., Kostygov, A. M., Petinov, V. I., and Chizhov, P. E., *Sov. J. Low Temp. Phys.* **1,** 674 (1975); *Phys. Rev.* **82,** 87 (1951).
13. Pfnuer, H., Feulner, P., Engelhardt, H. A., and Menzel, D., *Chem. Phys. Lett.* **59,** 481 (1978).
14. Madey, T. E., Engelhardt, H. A., and Menzel, D., *Surf. Sci.* **48,** 304 (1975).
15. Anton, R., Heinemann, K., and Poppa, H., *Proc. Int. Vac. Congr. 8th,* **1,** 121 (1980). Supplement to "Le Vide, les Couches Minces" (F. Abélès and M. Croset, Guest Eds.), No. 201 Suppl. Cannes, France, 1980.
16. Ruckenstein, E., and Chu, Y. F., *J. Catal.* **59,** 109 (1979).
17. Wang, T., and Schmidt, L. D., *J. Catal.* **66,** 301 (1980).
18. Heinemann, K., Osaka, T., and Poppa, H., *Ultramicroscopy* **12,** 9 (1983).
19. Heinemann, K., Osaka, T., Poppa, H., and Avalos-Borja, M., *J. Catal.* **83,** 61 (1983).
20. Doering, D. L., Poppa, H., and Dickinson, J. T., *J. Vac. Sci. Technol.* **20,** 827 (1982).
21. Broden, G., Rhodin, T. N., Brucker, C., Benbow, R., and Hurych, Z., *Surf. Sci.* **59,** 593 (1976).
22. Blyholder, G., *J. Phys. Chem.* **68,** 2772 (1964).
23. Doyen, G., and Ertl, G., *Surf. Sci.* **43,** 197 (1974).
24. Van Hardeveld, R., and Hartog, F., *Surf. Sci.* **15,** 189 (1969).
25. Singh, K. J., and Grenga, H. E., *J. Catal.* **47,** 328 (1977).
26. Goodman, D. W., Delley, R. D., Madey, T. E., and White, J. M., *J. Vac. Sci. Technol.* **17,** 143 (1980).
27. Rabo, J. A., Rish, A. P., and Poutsma, M. L., *J. Catal.* **53,** 295 (1978).
28. Herring, C., *Phys. Rev.* **82,** 87 (1951).
29. Lee, H. I., Praline, G., and White, J. M., *Surf. Sci.* **91,** 581 (1980).
30. Reed, P. D., Comrie, C. M., and Lambert, R. M., *Surf. Sci.* **64,** 603 (1977).
31. Lee, H. I., Koel, B. E., Daniel, W. M., and White, J. M., *J. Catal.* **74,** 192 (1982).